

## Workflows in a Virtual Morphology Lab: 3D scanning, measuring, and printing

Markus Bastir<sup>1</sup>, Daniel García-Martínez<sup>1</sup>, Nicole Torres-Tamayo<sup>1</sup>, Carlos A. Palancar<sup>1</sup>, Francisco Javier Fernández-Pérez<sup>1</sup>, Alberto Riesco-López<sup>1</sup>, Pedro Osborne-Márquez<sup>1</sup>, María Ávila<sup>2</sup> & Pilar López-Gallo<sup>3</sup>

1) Paleanthropology Group, Department of Paleobiology, Museo Nacional de Ciencias Naturales, (MNCN-CSIC). J. G. Abascal 2, 28006 Madrid, Spain

e-mail: mbastir@mncn.csic.es

2) Bellas Artes, Universidad Complutense Madrid, Calle Pintor el Greco, 2, 28040 Madrid, Spain

3) Comunicación y Programas Públicos, Museo Nacional de Ciencias Naturales (MNCN-CSIC); J. G. Abascal 2, 28006 Madrid, Spain

**Summary** - *The aim of this paper is to give a practical overview, showing how recent available digital technology can be combined to build a laboratory capable to produce 3D (and reproduce in 3D) anatomical models for research, teaching and museum exhibitions on topics related to anatomy, morphology in natural sciences, biology and medicine. We present workflows in our Virtual Morphology Lab that can be used for research, training (museum, academic), and external service. We first review different surface scanning equipment and post-processing techniques that are useful for scanning in museum collections and provide technical recommendations for hard- and software as well as storing media on the web. This section is followed by an overview of available software packages for rigorous and effective 3D measurements of landmarks and sliding semi-landmarks, providing extensive supplementary information with guiding manuals for self-teaching in these cutting-edge but complicated research methods. We review briefly most recent work on virtual GM and describe ways for representing results in form of 3D images and 3D prints (outputs). The last part is dedicated to a summary of our experience in 3D-printing using FDM technology of differently sized printers and thermoplastic materials. Finally, we discuss the above-described workflows and its potential applications in research (paleo, biomedical), teaching and museums pedagogics.*

**Keywords** - 3D analysis, 3D printing, Digital laboratory, Virtuality, Digital paleoanthropology.

### Introduction

Since the first studies have applied medical imaging techniques (computed tomography, CT) to the digital study of hominin fossils (e.g., Spoor *et al.*, 1994; Zollikofer *et al.*, 1995; Conroy *et al.*, 1998) continuous technological advances have complemented available methods for digitisation of anatomical structures. Among radiological methods high resolution industrial CT scanning (microCT) (Fajardo & Müller, 2001) and cone-beam CT (Maret *et al.*, 2010) have been applied increasingly to questions in physical and evolutionary anthropology and have facilitated insight into internal bone features. On the other hand, external

features can be digitised by surface scanning and during the last decade laser scanners, optical scanners or photogrammetry have become increasingly easily available (Mikhail *et al.*, 2001; Bruner & Bastir, 2008; Niven *et al.*, 2009; Sellers *et al.*, 2009; Friess, 2012; Guidi *et al.*, 2014; Weber, 2015; Fau *et al.*, 2016; García-Martínez, 2017). The technological advances have not only made these devices more and more affordable but, by producing digital collections of fossils (Bruner & Bastir, 2008), these advances have also initiated a change in the paradigm how morphological research is being carried out in human palaeontology and how fossil data can be accessed, distributed, and shared (Weber, 2001; Berger *et al.*, 2015).

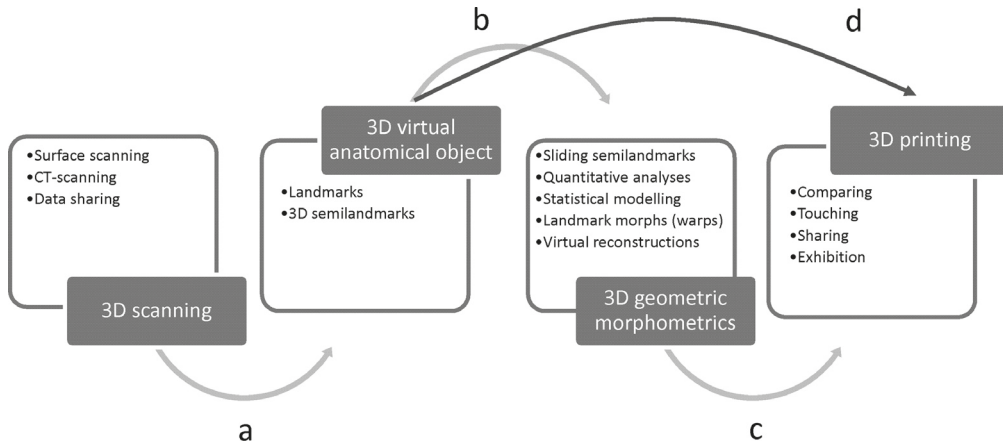


**Fig. 1 - Typical workflow of processes in a Virtual Morphology Lab. The first step is the digitalization of anatomical objects. The scanning process (a) produces 3D virtual objects that can be stored (and shared) in digital collections. Virtual 3D models are the input source, on which 3D landmarks and semilandmarks can be measured (b). These landmarks and semilandmarks can be processed and analysed using the geometric morphometric (3D-GM) toolkit for statistical analysis of object geometries characterised by curves and surfaces through semilandmarks. The graphical results of the 3D-GM analysis can be 3D printed (c) and manipulated for further morphological exploration, or exhibition. (d) Alternatively, after scanning a virtual anatomical object can directly 3D-printed for manipulation.**

The above mentioned technological developments are of particular importance for palaeo-anthropology and this is based on two reasons: on the one hand, global economic trends tend to limit grants for basic science and make travelling for accessing fossils difficult, particularly for younger students who carry out their MSc or PhD research without funding (Catanzaro, 2010; Pain, 2012). On the other hand, the process of measurement has changed from quantifying angles or distances to measuring complex spatial configurations of 3D landmarks and semilandmarks for rigorous 3D morphometrics (Mitteroecker & Gunz, 2009).

In anthropology, these methodological advances have become known as “Virtual Anthropology” (Recheis *et al.*, 1999) and when extended to a more generalized morphological research (palaeontology) these have been termed “Virtual Morphology” (Weber, 2015). The last decades have seen an explosion of studies using virtual morphological methods and have often changed the way one comprehends morphological changes in development and evolution (Recheis *et al.*, 1999; Weber *et al.*, 2001;

Zollikofer & Ponce de León, 2005; Dedouit *et al.*, 2007; Kullmer, 2008; Weber, 2015; Weber & Bookstein, 2017). In addition, open source code for 3D-GM has further pushed its application to very different kinds of data, to personalize the analyses, and have led to a generalized understanding of the importance considering 3D features of morphological structures (O’Higgins & Jones, 1998a; Slice, 2000; Klingenberg, 2011; Schlager, 2017).

More recently, also 3D printing has entered into basic workflows of this virtual morphological machinery (Fig. 1) (Zollikofer & Ponce de León, 2005; Jones, 2012; Bastir *et al.*, 2019). So far 3D printing is mostly used to reproduce previously digitised bones (Carew *et al.*, 2019). However, 3D printing also links perfectly with an extended workflow that includes 3D-GM. With 3D printing, the analytical process from 3D data acquisition, 3D data analysis and modelling, the researcher extracts information from the real world to model this information in the computer (virtual world) and then, produce again real-world physical outputs for comparison with other real-world specimens (Bastir, 2018),

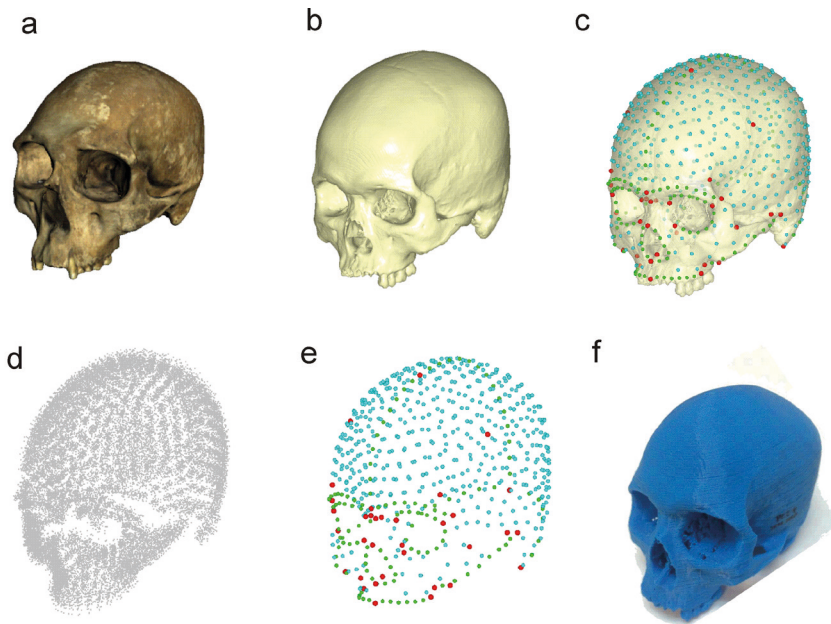


**Fig. 2 - Illustration of different steps and processes in a Virtual Morphology Lab. (a) Real cranium, (b) virtual 3D model of a cranium, (c) 3D landmarks (red) and semilandmarks of curves (green) and surfaces (blue) on a semi-transparent virtual cranial model. (d) Procrustes registered 3D landmarks and semilandmarks of a large sample. (e) Mean shape of this sample. (f) 3D PLA-printed cranium warped to the mean shape of the sample. The colour version of this figure is available at the JASs website.**

for physical manipulation, comprehension and, finally, for communication (Fig. 2). Particularly in the context of communication, this technology becomes important not only for academic but also for museum education, pedagogics and activities (Canessa *et al.*, 2013; AbouHashem *et al.*, 2015; Lim *et al.*, 2016).

The aim of this text is to describe, from a less theoretic and more practical point of view, the main processes and to overview basic infrastructural needs in order to build a Virtual Morphology Lab for paleoanthropological, or more generally, morphological research and for transmission of knowledge and communications in Natural Science museums. Importantly, while the workflows described here are general, the infrastructural details of the lab described later in this paper are specific to our lab and show only one of many different ways to implementing these technologies for morphological research and museology.

## The acquisition of digital 3D surface models in osteological collections

### *3D surface scanning process*

The aim of this section is to describe main steps in 3D-surface scanning using portable equipment that can be carried easily travelling to osteological collections. Therefore, here we focus on descriptions and handling suggestions of our equipment of small-sized (Next Engine HD Laser scanner) and hand-held (Artec Spider, MHT, EVA) scanning devices. These surface scanners are widely used in physical anthropology and palaeoanthropology and are accurate for obtaining high-resolution 3D models that can be used for 3D-GM analyses in the scope of anthropology, but also for imaging based teaching in comparative anatomy classes and workshops in natural sciences museums. While here basic and practical features will be described, other

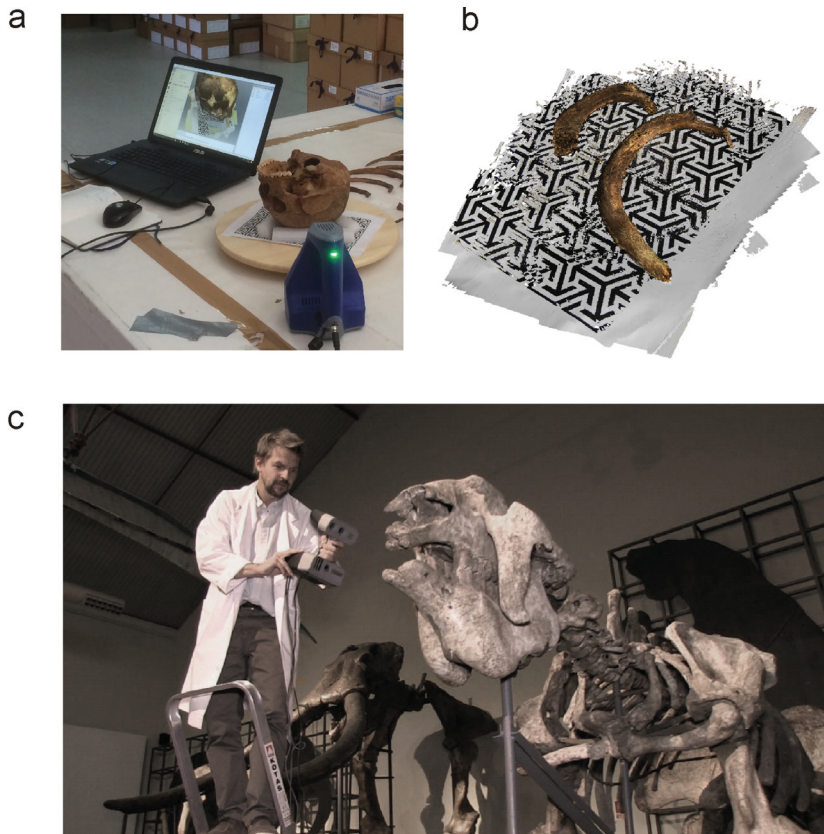


**Fig. 3 - Scanning processes. (a) Typical set up for 3D surface scanning in a museum collection showing the scanner, the laptop computer, and the turntable. Note that we fixed a texture pattern sheet on the turntable to improve texture tracing during the scanning process. (b) Virtual image of two ribs and the texture pattern sheet after scanning. The black-and-white geometries improve the speed as it facilitates recognition of subsequent scans. This is helpful when the anatomical object offers only few easily recognisable anatomical details (curved ribs, bones of the neurocranium, long bone shafts, etc.). (c) Scanning very large objects (Megatherium americanum of the MNCN, Madrid) with a hand-held scanner requires powerful computers and graphic cards both during scanning and for post-processing. The colour version of this figure is available at the JASs website.**

publications (e.g. Friess; 2012; Katz & Friess; 2014) provide detailed technical information on surface scanning technology.

Surface scanners are optical systems that can be used for measuring anatomical objects through visible light to generate dense 3D polygonal meshes (Friess, 2012). Most frequently these scanners are based on laser, white, or other structured light sources. A source light is emitted, reflected by the object and the reflection detected again by the cameras of the scanner. Specifically,

and as outlined by Friess (2012), most surface scanning methods use the principle of triangulation of the x, y, z-coordinates of the light reflection (on the anatomical structure being scanned) on the basis of the known distance and angle between emitted and received light. When this recording is carried out successively and from different angles, more and more x, y, z-coordinates of measurement points are recorded giving rise to a geometric representation (by 3D points) of the anatomical object.

There are several methods that can be used to get such point clouds of osteological objects which depend basically on the size of the object, its geometrical complexity and surface features. Two principal methods are available in our lab: Laser scanning with a NextEngine HD scanner and structured light scanning with Artec scanners. The laser scanner emits laser beams which are reflected by the surface of the object and this reflection is captured by the camera of the scanner. The object rotates on a turntable and each position of the turntable gives rise to a single scan (the researcher can select the angular intervals, the number of scans). After a full rotation, all the scans are aligned automatically to produce an (optionally) textured 3D surface model, which can be edited (cleaned, simplified), in the associated software relatively quickly. This is practical as it enables the researcher to do other work on the collection while scanning, but it is also a slow process. Depending on the number of scans selected (6-7 scans), the scanning process lasts about 10 minutes each full rotation. Usually the bone needs to be scanned at least in two different positions to digitize all the surfaces of the object, which is a problem when a large number of bones needs to be scanned. For example, for scanning serial elements such as ribs (García-Martínez *et al.*, 2018), we designed a fixation device, which enabled us to scan six ribs at a time saving time. However, the post-processing of these scans was more tedious, and the total time consumed for each rib was about 15 minutes. This helps accelerate the scanning procedure in the osteological collection and saves travel time because post-processing can be done later in the hotel room or back in the lab.

With hand-held scanners there is usually no automatic turntable, but rather the digitizing person (=digitizer) must change the spatial position of the scanner with respect to the object by moving the device manually over the object (Fig. 3a). When scanning small-to-medium sized objects with the hand-held device, we use turntable that can be rotated manually in relation to the geometric complexity of the anatomical object. While with the laser scanner the angles between the rotations of the object on the turntable are

fixed and are used to generate geometric continuity between the scans, Artec Studio software can use both geometry and texture to keep the continuity between different scans. Scanning speed depends on the capability of the system to keep track of the object continuity between each frame (3D-image) when the scanner is moved over the object, or the object itself is rotated on the turntable. Also the scanning rates contribute to scanning speed. These rates range from 6-8 frames per second in case of the Artec (Space) Spider scanner and up to 20-30 frames per second in the Artec EVA (before MHT) scanner ([www.artec3d.com](http://www.artec3d.com)). In the Artec Studio 12 software, activating the texture tracing option contributes further to a fast and precise scanning process. Texture tracing works better by putting a paper sheet with a graphic pattern below the object to be scanned (Fig. 3b). This provides additional textural information and helps the scanner to keep track of the geometric continuity of the object scan between each frame. If continuity is lost, the scanning software emits a warning signal and the digitizer can re-adjust. The scanner “waits” a bit until the last scanning position for which continuity can be achieved, is obtained. Therefore it is useful not to scan too fast, despite the temptations offered by the technological possibility.

Typically, with the Artec Spider scanner, the time for digitizing smaller bones, such as vertebrae, foot or hand bones ranges between 3-6 minutes from scanning to semi-automatic 3D reconstruction using Artec Studio 12. The scanning of intermediate-sized bones (e.g. mandible, hipbones, and sacrum) can take about up to 10-15 minutes. Scanning the skull or long bones such as a femur or tibia, can take a bit longer because of their more complex geometry, but experienced users can keep scanning time around 15-20 minutes. In larger object also the post-processing times can increase considerably. (Importantly, scanning too long with the Artec Spider equipment could also lead to failure of texture LEDs and the need for repair.)

Of particular challenge is the scanning of curved objects (ribs or partial neurocrania, for

instance) where little geometric references are available. Here the use of additional objects (and their geometries), or the above mentioned texture features can help. Consequently, scanning of triplets of ribs is easier and faster than scanning them individually. Post-processing, however, will take longer as the different bones need to be reconstructed separately. In very large objects, also the hardware (graphics card, working memory and processor speed) is important. Powerful computers are necessary during scanning because a large number of points on the surface of the object (point cloud) are collected, which serves as a set of vertices in a common 3D coordinates system and represents the external surface geometry. When triangulated, these points are connected by small continuous polygons giving rise to a closed overall surface mesh reflecting the geometry of the object (Friess, 2012). Scanning big objects with large point clouds produces many polygons (Fig. 3c). The processing of these, which is achieved via mathematical algorithms, requires high processor capacities and working memory (graphic cards, RAM).

Both techniques are well suited for scanning in osteological collections although laser scanning gets a bit more difficult with larger objects that do not fit the turntable. However, in this latter case it is possible to scan, statically, different views of the large object and then fit these surfaces together manually. Even so, if time is an issue, our experience suggests that hand-held devices are preferable. In our opinion, the best combination is to use Artec Spider for scanning small to medium sized objects (e.g. human phalanges, mandible, humerus) and Artec EVA for larger bones such as entire crania, femora, or fused pelvis, or even very large objects (Fig. 3c). However, in Artec scanning software both devices and their 3D scans can be combined. This way, one could scan the bigger structures with EVA and the more detailed parts with the Spider and fuse these images.

#### *Post-processing and finalising 3D meshes*

Despite the fact that digitisation quality is usually high, any scanned object must be

considered a reproduction of the real object and some processes and parameters are crucial to keep the level of accuracy as high as possible. Standard processes include the alignment of different scans, hole-filling, small object filters, smoothing and mesh simplification. Most software packages of scanning equipment offer these options (e.g. NextEngine ScanStudio, Artec Studio). Also, free software, e.g. Meshlab (Cignoni *et al.*, 2008), Rvcg (Schlager, 2017) or commercial packages (Geomagic) can be used for carrying out some of these tasks.

The alignment is the process by which all 3D scans are combined into a single 3D model. There are several methods (drag, automatic, manual, etc. ...) of alignment and all of them are useful; the clue is to be sure the alignment has been done properly and the model has no inconsistencies, scars or distortions in the alignment plane. This is usually followed by finding and filling smaller holes or bigger edges in the surface. Closing the holes of the surface mesh is important because, during 3D-GM procedures (see **Measurement of 3D meshes (landmarks, semilandmarks of curves and surfaces)**), in particular during the process of sliding semilandmarks, these points could move inside the 3D model through these holes and lead to problems. In addition, for 3D printing the slicing software requires closed (water-tight) 3D models.

Another standard mesh cleaning process is the application of a small objects filter. Specifically in osteological collections or other environments with dust and in combination with higher scanning sensitivity, small particles can cause light reflection artefacts and a kind of background noise that show up as tiny, sometimes disconnected surface irregularities. Small object filters usually detect and remove these.

Smoothing and decimation (mesh simplification) are two more delicate problems in the post-processing stage (Veneziano *et al.*, 2018). Surface smoothing is a re-arrangement of the vertices of the mesh rendered on the basis of the point clouds. Smoothing reduces the noise caused by scanning artefacts, such as light reflection, that is sometimes observed on the surface of the bone.

However, several smoothing algorithms are available producing different kinds of artefacts and some guidelines for their minimisation have been published recently (Veneziano *et al.*, 2018). According to these it seems that smoothing is more important for getting realistic 3D prints rather than for obtaining accurate 3D measurements.

Decimation, or mesh simplification, is the reduction of the number or triangles in a mesh. 3D models with higher resolution can easily be reduced to about 50%. However, Veneziano *et al.* (2018) suggested that, by definition, decimation should be kept low and should be applied selectively to the regions of interest, as different parts of an object could be affected differently by the same parameters of decimation. However, because mesh simplification reduces the size of the 3D model, the digital handling can be improved considerably (Fig. 2e), which is particularly useful for inspection and interactive warping and visualization of 3D meshes in 3D-GM software (see below).

Finally, “rescale” is an interesting tool for 3D printing an object in a size different to the original one, which may be useful for educational or dissemination purposes. Rescaling allows for increasing the size of a small object, or reducing the size of a very large one. Rescaling contributes to better understanding of tiny structures for example in museum workshops working with children or pupils.

Running through all these post-processing steps leads to producing an accurate and lightweight 3D model that contains an accurate geometry of the original object ready for measurement, analyses and 3D-printing.

#### *Databases on the internet*

The digitization of fossils or other anthropological material creates new perspectives with regard to the sample storage, curation and access. There are several online databases storing all kind of extant and fossil remains, and making them broadly available for research or educational purposes. This fact has greatly transformed the world of palaeoanthropology, giving it a global breadth of access, making it easier for any research team

to study material (Berger *et al.*, 2015; Boyer *et al.*, 2016; Copes *et al.*, 2016; Seiffert *et al.*, 2016). Digitally accessible data bases speed up research enormously as it is possible to access the object whenever necessary via internet, and it is possible to work not only virtually, but also with a physical version of the virtual models using 3D printing (see **3D printing of virtual morphological objects and 3D-GM results**). It contributes to conservation as any risk of potential damage to the original object due to manipulation is avoided. No travelling is necessary to get the sample, reducing costs, which is particularly important for younger researchers. However, it should be noted that in some respects (finer morphological details, etc.) a digital model cannot replace originals and complementing research with original descriptive literature, and research quality casts is highly recommended. Table 1 shows a list of the most complete anthropological databases and their particularities.

### **Measurement of 3D meshes (landmarks, semilandmarks of curves and surfaces)**

#### *Introduction to landmarks and semilandmarks: the quantification of shape*

Geometric morphometrics is based on the quantification of the shape of a structure, which is captured by Cartesian coordinates collected from specific anatomical points (landmarks) in a two-dimensional or three-dimensional space (Bookstein, 1991). These landmarks are biologically homologous in all the individuals of the sample. One of the great advantages of this method is that it allows a statistical analysis of size and shape separately since in GM the morphology of an object is decomposed into size and shape (Zelditch *et al.*, 2012). According to the traditional definition of Kendall (1977), shape is “all the geometric information that results from eliminating the effects of the position, scale and rotation of an object”. This is achieved by applying translation, scaling and rotation to the landmark configurations which guaranties that the relative positions between the

**Tab. 1 - List of the most complete anthropological databases.**

NAME	WEBSITE	TYPE OF DATA	FORMAT	COST
Virtual Anthropology	<a href="http://www.virtual-anthropology.com">www.virtual-anthropology.com</a>	Fossil hominoids	CT-Scans	Yes
African fossils	<a href="http://www.africanfossils.org">www.africanfossils.org</a>	Hominid, animal and tool models from the African continent	Surface scans	No. Creating an account is necessary.
Digital Morphology	<a href="http://www.digimorph.org">www.digimorph.org</a>	Paleontological models	STL and/or CT-Scans	No
NESPOS	<a href="http://www.nespos.org">www.nespos.org</a>	Extant and fossil hominins and primates	STL and/or CT-Scans	No. Creating an account is necessary.
EVAN Archive	<a href="http://www.evan-society.org">www.evan-society.org</a>	Fossil samples, including skulls and postcranial elements.	CT-Scans and surface scans	Yes
ORSA	<a href="http://www.penn.museum/sites/orsa/Welcome.html">www.penn.museum/sites/orsa/Welcome.html</a>	Human and non-human skulls	CT-Scans	No
Morphosource	<a href="http://www.morphosource.org">www.morphosource.org</a>	Current and fossil remains	Surface scans and micro-CT	No. Creating an account is necessary.
KUPRI	<a href="http://dmm.pri.kyoto-u.ac.jp/dmm/WebGallery/dicom/researcherTop.html">http://dmm.pri.kyoto-u.ac.jp/dmm/WebGallery/dicom/researcherTop.html</a>	Extant primate body cadavers	CT-Scans	No. Creating an account is necessary.

landmarks do not change, while the absolute position does. This superimposition allows to study the “pure” form of an object (Kendall, 1977) and is called Procrustes superimposition (Zelditch *et al.*, 2012). This superimposition yields Procrustes shape coordinates as measures of 3D shape. Size is quantified in GM as “centroid size” (CS), defined by the square root of the sum of the distances squared from the landmarks to their centroid (Zelditch *et al.*, 2012). The centroid is the average of the x, y and z coordinates of all landmarks.

Regarding landmarks, traditionally three different types of landmarks have been defined according to their spatial location: type 1 (juxtaposition of tissues), type 2 (local properties such as maximum of a curvature) and type 3 (extremal points, or constructed landmarks) (Bookstein, 1991). These categories define the quality of information provided

by such kinds with type 1 providing more biologically relevant information than types 2 and 3. Constructed landmarks have more recently defined by categories such as “pseudo- or semi-landmarks” (Bookstein, 1991, 1997; Dryden & Mardia, 2000). Semilandmarks are pseudolandmarks that are processed further mathematically (re-sliding, see below). However, recent trends avoid the typology of classical GM and use only the terms “landmark”, for measurement points that are clearly discernible (old type 1). For complex anatomical structures that lack Type 1 landmarks, and thus, where definition and homology of the measurement points in a sample is “deficient” or somehow else questionable, e.g. rib curvature or the neurocranial surface or the neurocranial surface, “curve semilandmarks” and “surface semilandmarks” are used (Gunz & Mitteroecker, 2013).

**Tab. 1 - continued**

NAME	PROPERTY	COMMENTS
Virtual Anthropology	University of Vienna (Vienna, Austria)	The data requested is sent on a CD-ROM with the original CT-Scans at a small price.
African fossils	Turkana Basin Institute, and the National Museums of Kenya, Stony Brook University and the National Geographic Society	You can previsualize the objects online, manipulate them and watch them with texture. The object's measurements and its scanning method (surface scanning, photogrammetry, etc.) are given
Digital Morphology	University of Texas (Austin, Texas, USA)	It is possible to contact the model's curator to obtain one (good treatment and fast response) if a model does not present the download option.
NESPOS	ART+COM, the Natural History Museum of London and the Neanderthal Museum of Mettmann, among others.	
EVAN Archive	European Virtual Anthropology Network	You have to become an EVAN-Society member. The annual fee is 100€
ORSA	Penn University Museum (Philadelphia, Pennsylvania, USA)	This website offers a list with the description of the skulls, with a historical tracking. The data demanded is sent on a CD-ROM or a DVD at a small price. It is possible to contact the curator to obtain the models that are not available online.
Morphosource	Duke University (Durham, North Carolina, USA)	In some cases, a request has to be sent to the curator of the model in order to download it. Some hominin fossils, such as <i>Australopithecus sediba</i> or <i>Homo naledi</i> were uploaded to this website
KUPRI	Kyoto University Primate Research Institute (Kyoto, Japan)	You can find detailed information about sex and age of the individuals. The objects can be previsualized online.

Semilandmarks are “deficient” because there is no clear criterion to define their exact position other than, “on the curve” or “on the surface”. Their best position is actually unknown as the curves or surfaces they should quantify lack anatomical details, which could be used for homologization. Other than a true landmark, which marks a biological and thus homologizable structure in a sample, all semilandmarks mark a homologous curve or surface *together*, that is, in their sum. A single semilandmark in isolation is meaningless. Thus, a problem exists as to how to establish a geometrical correspondence (or homology) among semilandmarks in a given sample (Gunz & Mitteroecker, 2013).

To solve the problem of deficient biological homology among the semilandmarks the sliding semilandmark methodology has been

developed (Bookstein, 1991, 1997; Gunz *et al.*, 2005, 2009; Gunz & Mitteroecker, 2013; Mitteroecker & Gunz, 2009; Toro-Ibacache *et al.*, 2010). These methods establish a geometrical homology between semilandmarks by means of mathematical algorithms that are used to optimise the positions (re-slide) of curve or surface semilandmarks. Two major different re-sliding (= repositioning) algorithms are used (Pérez *et al.*, 2006; Gunz & Mitteroecker, 2013): 1) re-sliding to reach the minimum energy of deformation (bending energy, BE) between a specimen with respect to a reference (Bookstein, 1991, 1996, 1997; Bookstein *et al.*, 2002) and 2) re-sliding to reach the minimum Procrustes distance between a specimen with respect to a reference (Sampson *et al.*, 1996, Bookstein *et al.*, 2002, Sheets *et al.*, 2004). The first approach is based on the sliding

during thin-plate-spline deformation (Bookstein, 1991) while the second approach is based on the Procrustes superimposition (Gower, 1977; Rohlf & Slice, 1990). Minimizing bending energy during the sliding process is particularly recommendable in the context of virtual morphology, where deformation of meshes is used for interpretation or 3D-printing, because minimizing BE leads to 3D models with smoothly interpolated geometries (Fig. 2).

The interpolation algorithm of the thin-plate-spline (TPS) deformation is borrowed from material sciences (Bookstein, 1991) and has been used to visualize differences in shape between two specimens in the sense of grid transformations introduced by D’Arcy Thompson (1917). In TPS methods the bending energy is quantified that is necessary to deform one set of landmarks (shape 1) in another one (shape 2). If two configurations differ strongly, or if this difference is in a localized region, higher bending energy is necessary to transform one configuration into the other than if two configurations are more similar to each other. The advantage of the TPS lies in its capacity for visualizing the deformations of shape, not only of 2D grids, but also of the 3D meshes associated with the set of coordinates. These deformations (typically called morphs or warps) make shape differences between two landmarks configurations very intuitive (see next section) even if the shapes and/or their differences are complex (e.g. Bastir *et al.*, 2011) (Figs. 2,4).

Procrustes distance between two specimens is quantified as the square root of the sum of the square distances between their homologous landmarks after Procrustes registration (Mitteroecker & Gunz, 2009). A greater Procrustes distance between two shapes will be defined by greater distances between homologous landmarks of those sets of coordinates and, therefore, it will mean a greater morphological difference.

These two methods are used in the re-sliding procedure during which the new positions are calculated (= estimated) for semilandmarks with only two criteria: criterion 1): minimising either the bending energy (BE) or Procrustes distances

(PD) between the first configuration and the reference (often the average shape, consensus) and criterion 2): being located on a curve or on a surface. By fulfilling these two criteria the positions of the semilandmarks after the resliding procedure can be considered geometrically (mathematically) homologous.

The main difference between both sliding approaches is that bending energy takes into account all the landmarks and semilandmarks to calculate the deformation energy as a whole or set, and the sliding of each semilandmark is influenced by the sliding of adjacent landmarks and semilandmarks. This introduces covariation among the semilandmarks. In the Procrustes distance minimization approach, each semilandmark does the sliding separately and is not influenced by the position of adjacent landmarks and semilandmarks. Therefore, potentially, when doing the resliding through the PD minimisation approach, it may happen that a semilandmark passes a landmark, which, through the BE minimisation method is impossible. Whatever the process used, for the sliding to be possible in mathematical terms, the semilandmarks of the curve must slide along lines tangent to these curves, while the surface semilandmarks slide along planes tangent to them (Gunz & Mitteroecker, 2013). Because of this curve semilandmarks have 1 degree of freedom due to their sliding along tangents and surface semilandmarks slide have 1 degree of freedom due to their sliding along tangent planes. Semilandmarks may lose their contact with the 3D surface because this would be the optimal position of minimal BE or PD (Criterion 1). However, in order to fit also Criterion 2 they must be re-projected onto the curve or surface again (Gunz & Mitteroecker, 2013).

It has been recommended to carry out the sliding process twice to optimize the position of the semilandmarks: first, taking (arbitrarily) any specimen of the sample to be digitized as a reference. This is usually the specimen on which the landmark template is based on (see below). Second, after all specimens have been measured their average shape (consensus) of the sample is

used as new reference against which the semilandmarks are reslid (Gunz *et al.*, 2009; Gunz & Mitteroecker, 2013). After all this process, a mathematical homology is achieved and the reslid semilandmarks can be treated as landmarks.

#### *Missing data estimation by the use of semilandmarks*

Finally, it should be noted that sliding semilandmarks methods are also very useful for the estimation of missing landmark data in incomplete structures (e. g. broken fossils, or part of fossils). Missing landmark estimation methods are necessary because geometric morphometrics only work if all specimens are represented by the same number of homologous landmarks. Thus, in broken or otherwise incomplete structures it is necessary to estimate the coordinates of the non-preserved landmarks. Anatomical, geometric and statistical estimation methods have been developed (Gunz *et al.*, 2009). Once the landmarks are estimated surface deformations (warps, morphs) can be used to generate, virtually, the missing 3D structure.

If a structure is missing that belongs to a symmetrical anatomical object, we can use mirror images to perform the reconstruction of the specimen (anatomy-guided missing data estimation) (Zollikofer *et al.*, 2005; Ponce de León *et al.*, 2008; Gunz *et al.*, 2009; Weber & Bookstein, 2011; O'Higgins *et al.*, 2011). However, when parts are absent on both sides or when a structure is not symmetric then other methods are necessary. The sliding algorithms can be used to estimate the positions of semilandmarks even when there are no surfaces onto which they can be projected. This method is called geometric and reference-based estimation of missing data (Gunz *et al.*, 2009). It is possible because during the regular semilandmark sliding process, the final position is previously unknown and only defined after the resliding procedure in a given sample. The positions of semilandmarks need always be estimated with respect to the sample and the anatomical structure either along the tangent line (curve semilandmarks) or the tangent plane (surface semilandmark). The difference between complete and

incomplete structures consists only in the fact that in the incomplete structure (e.g., a broken fossil), no surface exists onto which the semilandmarks could be projected but the position of the semilandmark itself can be estimated. Importantly, the more landmarks and semilandmarks are located close to the missing structure, the more morphological information will be exploited and the more reliable the estimation of missing structures will be (Gunz *et al.*, 2009; Gunz & Mitteroecker, 2013). Further certainty in the estimation of missing data can be gained by creating different estimates using different possible references or methods [anatomically guided reconstructions, statistical reconstructions (Gunz *et al.*, 2009)]. This way, several different estimates of the same structure can be produced following different methods and/or hypotheses. Consequently, different reconstructions are available for analysis and any possible bias or reconstruction-artefact can be assessed (Gunz *et al.*, 2009, Neubauer *et al.*, 2018). Obviously, these geometric morphometric reconstruction techniques are very attractive when combined with 3D printing because this converts a fragmented anatomical structure in a complete one that has been reconstructed on a quantitative basis and can further be manipulated (Fig. 1).

#### *Basic analyses in geometric morphometrics*

3D-GM analyses are based on the study of the size and shape extracted from landmark configurations in a sample. To obtain the array of 3D coordinates two main options exist: on the original object or on a virtual 3D model of the original object, which has to be previously obtained using digitization methods (see **The acquisition of digital 3D surface models in osteological collections**). If landmark coordinates are to be collected on the original physical object, a digitizing tool is needed. One of the most extensively used tools recently is the MicroScribe device. It is a counterbalanced mechanical arm which allows the user to collect 3D landmark coordinates of an object using a sharp stylus. The 3D coordinates can be automatically pasted into an excel file while digitizing with a footswitch (Inscribe software). The MicroScribe digitizer also allows the user

to collect pseudolandmarks along a curve (ridge curves) or on a surface. In the latter a different pointer (ball tip) is recommended. This rounded stylus can be moved along the curve or surface collecting hundreds of semilandmarks without damaging the bone surface. Curve semilandmarks can be transformed into equidistant semilandmarks (for example, using the software “Resample.exe”). Importantly, the stylus should be always held orthogonally during landmark recording to the surface because rotations affect the coordinates. These curve semilandmarks can then be submitted to resliding in Viewbox 4.0.1.7 software, as recently shown in Rodríguez-Pérez *et al.* (2017). Surface landmarks need to be post-processed by more specific routines, for example those available in R (R Core team, 2017).

If landmarks coordinates will be collected on a virtual 3D model, two frequently used programs are available: Landmark editor or Viewbox 4.0.1.7. Landmark editor can produce data matrices of landmarks of curves and surfaces on virtual objects but the sliding of semilandmarks needs to be carried out in other programs (R Core team, 2017). In turn, Viewbox 4.0.1.7 is a commercial software (that can also be used licence-free with a bit of patience) for 3D data preparation, including basic edits of 3D surface meshes, or extracting meshes from CT-scans through segmentation, but also 3D landmark measurements and sliding of curve and surface semilandmarks, as well as basic geometric morphometric analyses including Procrustes superimposition, principal components analysis, Thin-Plate-Spline visualization and geometric methods for missing landmark data estimation. The supplementary information shows how to use Viewbox 4 to measure 3D landmark and semilandmarks on virtual 3D objects, how to carry out the sliding of the semilandmarks and the re-sliding to the sample mean, and how to produce reference-based missing data estimations based on the considerations laid out in section *Introduction to landmarks and semilandmarks: the quantification of shape*.

Once all virtual 3D specimens are digitized, a file with all 3D landmark coordinates of all the specimens is generated that, appropriately

formatted, can be imported in a large number of existing 3D-GM software depending on the analyses to be performed. MorphoJ (Klingenberg, 2011), Morphologika v2.4 (O’Higgins & Jones, 1998b), Morpheus *et al.* (Slice, 2000), IMP-software (Zelditch *et al.*, 2012) or Evan-Toolkit (ET) (Evan Society, 2010) are among the most widely used packages. NTS format is useful even in 3D because it works well in data base functions of tpsUtil software. However, a growing number of geometric morphometric analyses are carried out using open-access codes programmed in R such as Geomorph (Adams *et al.* 2019) and Morpho (Schlager, 2017).

The first step in any geometric morphometric analysis is the Procrustes superimposition (Fig. 4a,b) (O’Higgins, 2000; Mitteroecker & Gunz, 2009; Zelditch *et al.*, 2012) and this step is usually followed by several standard analyses. Most frequently a principal components analysis (PCA) is carried out (Fig. 4c), which helps to explore and visualize the major patterns of variation (Fig. 4d). Principal components analysis in GM is, however, not well-suited to test directly for hypotheses (Bookstein, 2017). This is related to the aim of the PCA, which is to reduce the number of variables in a data set by factors (principal components) that account for as much as possible of variance. A specific biological signal maybe, however, too subtle to be reflected in any of those principal components and thus it could not be detected. A specific version of PCA, the Procrustes Form Space PCA, can be used to analyse allometric trajectories for comparative growth analyses (Mitteroecker *et al.*, 2004; Bastir *et al.*, 2007).

Other typical analyses are mean comparisons, to address the question of differences in shape between different groups. These can be carried out either on the PC-scores obtained previously for parametric statistical analyses (PAST; Hammer, 2015) or directly on the shape coordinates using permutation approaches such as implemented in MorphoJ (Klingenberg, 2011) or Morpheus *et al.* (Slice, 2000).

The association between shape and a continuous factor (e.g. age, size, stature, temperature, etc.)

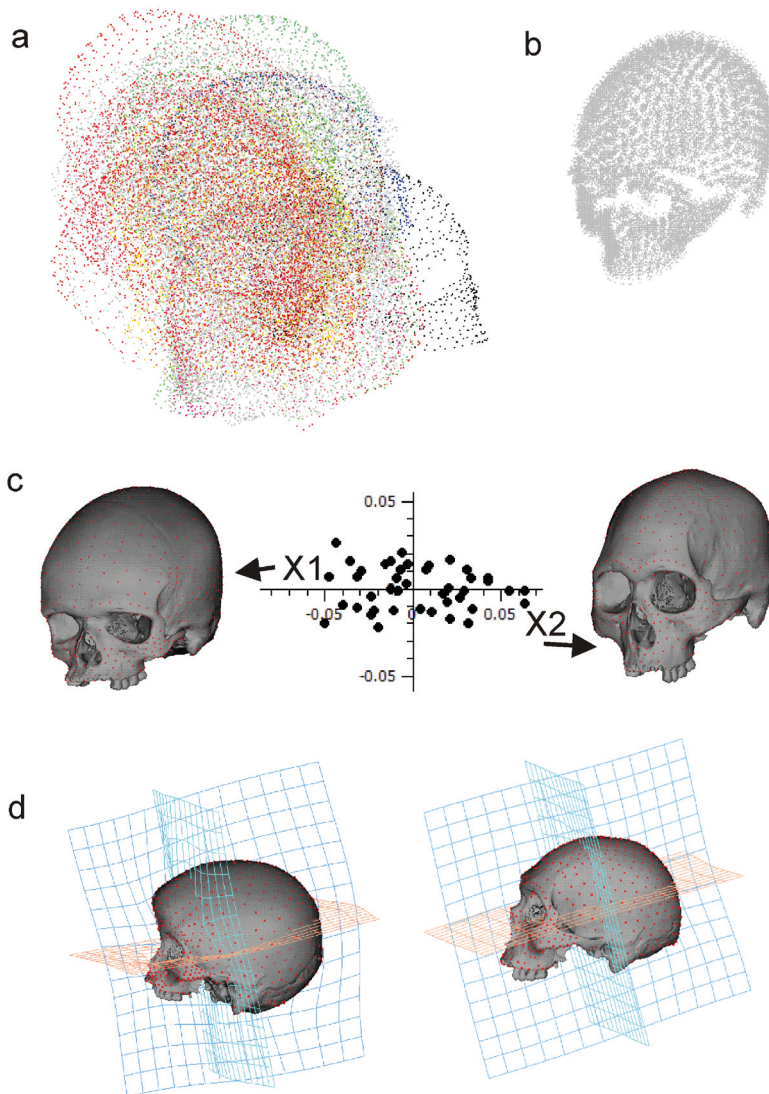


**Fig. 4 - Basic steps in a virtual 3D geometric morphometric analysis. (a) Many different crania in their natural positions after their landmark digitization using the landmarks template shown in Figure 2b. (b) Procrustes registered crania; (c) Principal components analysis as example for a first typical data exploration. We used the template skull in EVAN toolkit as warping reference to illustrate the variation along the shape vector of the first principal components. However, when shape variation is larger, or different species are used then warping to the endpoints of a given shape difference vector can be unrealistic due to large mesh distortion. In such cases those specimens should be used for warping that are most closely located to the end point of the vectors. (X1 mesh warped to the shape of the negative end of PC1 vector, and X2 mesh warped to the shape of the positive end of PC1 vector). (d) The same surface warps shown with Thin-plate spline grids in principal anatomical planes to aid understanding of specific features of variation. The colour version of this figure is available at the JASs website.**

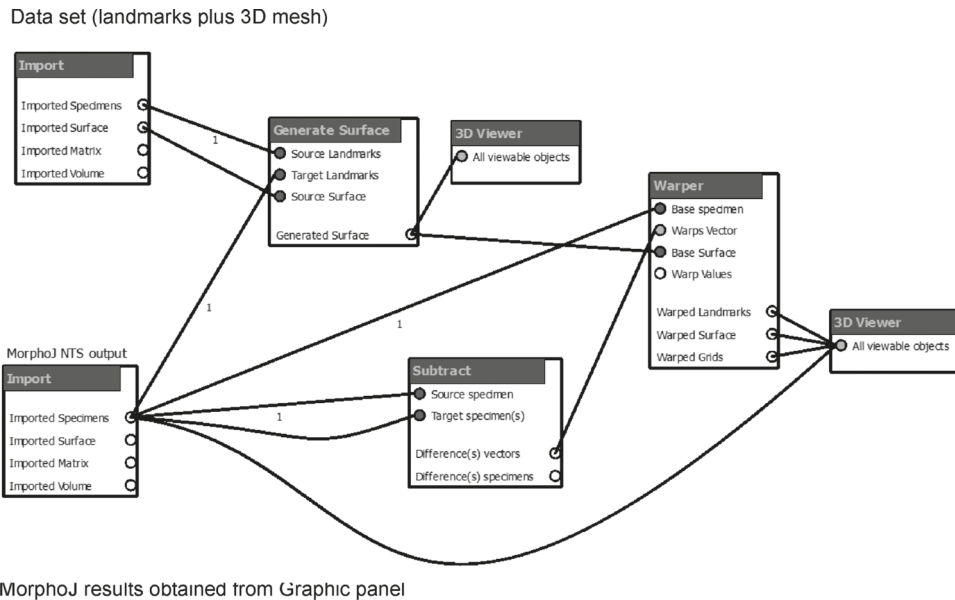


**Fig. 5 - MorphoJ warper.** This network uses the coordinates that can be exported from the graphic panel of MorphoJ to warp a 3D mesh along the vector defined by the coordinates in EVAN Toolkit. In the upper part of the network the original data set and a specific 3D mesh (that corresponds in space to the 1st specimen of the landmark file) are imported. In the lower part the landmarks to be visualized (e.g. MorphoJ results) are imported. This is a coordinate file (here in nts format) that consists of two configurations: a source (configuration 1) and a target (configuration 2). This network transforms original surface mesh to fit the landmarks of the MorphoJ results and the warper allows for interpolation between two landmark configurations obtained from MorphoJ.

is addressed by a multivariate regression analysis. MorphoJ and ET-software offer such options. ET also offers an option to predict the shapes of such regression models for a given value of the independent variable and to export these “standardised” shapes. However, if many landmarks and semilandmarks are used in a smaller sample the results of these regression analyses should be accompanied and checked with further regression analyses carried out on the PC scores (Mitteroecker & Bookstein, 2011).

The association and covariation patterns between two different shapes (e.g., face and neurocranium) can be studied by Two Blocks Partial Least Squares analysis (2B-PLS), that finds linear combinations in each block by maximising the covariance between blocks (Rohlf & Corti, 2000; Bookstein *et al.*, 2003). When applied to two sets of shape data, this method examines the

covariation through two different approaches (between separate blocks, and within-blocks).

A 2B-PLS between separated blocks (Bookstein *et al.*, 2003; Torres-Tamayo *et al.*, 2018) relies on separated Procrustes fits for each block and quantifies pure covariation in their shapes (e.g., pelvis and rib cage). In a within-configuration PLS the blocks of landmarks are defined within the entire configuration (Bastir & Rosas, 2016). This covariation is influenced not only by the variation of the shapes, but also by variation in the relative sizes, positions or orientations of the blocks. Thus, while the between block PLS could underestimate biological covariation, the within-block PLS could overestimate it. Therefore, it depends to some degree on the question which PLS approach is chosen and as a general recommendation on 3D-GM, many different analyses should be explored before final conclusions are made.

All these geometric morphometric analyses should be accompanied by 3D visualizations to link the statistical analyses with the corresponding morphological (graphical) information. Although the software packages mentioned above offer some kind of visualization it should be mentioned that to facilitate comprehension, interactive warp visualizations are preferable. Interactive exploration (that is, moving the pointer with the mouse along statistical vectors such as PC-axes, mean shape differences, or regression vectors) of 3D-GM results favours comprehension and is highly recommended.

When working with MorphoJ the 3D visualization is limited. However, a simple transformation of the coordinates, as output file of the MorphoJ Graphics panel, together with a specific network of ET-software (Fig. 5) converts the static graphical output of MorphoJ into an interactive, dynamic and heuristically powerful visualization.

With the network shown in Figure 5 any 3D surface mesh (.ply, .obj, .stl) can be deformed in ET so as to fit the shapes of the results of a MorphoJ analysis. To achieve this, two steps are necessary: First, load a coordinate data set with its corresponding 3D mesh (e.g., the 3D mesh of ViewBox template and the landmark coordinates of the template; or any other data set that contains landmarks of which one fits to a given 3D mesh) into the import node of ET shown in the upper part of Figure 5. Then load the coordinates of the results of any MorphoJ analysis. To obtain these coordinates right-click in the Graphics panel in MorphoJ and select “Export Coordinate File”. Then adjust the existing header text to the necessary header of the NTS format by 1) removing the first lines of text, 2) by defining the labels so as to specify the MorphoJ results, and 3) by replacing the missing landmarks codes from the default setting of MorphoJ “1 9999” to “0”, which is recognized by ET-software after the NTS data import). These edits can be done in any text editor. Then, load this NTS file into the Import node shown in the lower part of Figure 5 and run the network. Importantly, visualize not only the 3D mesh but also the proper landmarks

of the MorphoJ results. This way one can be sure to display exactly the kind of shape data that is of interest by the Warper node. The warper uses 3D TPS for transforming (morphing) the 3D mesh along the MorphoJ results.

ET-software provides further facilities for interactive visualization using different kinds of 3D glasses (e.g. shutter glasses, anaglyphic glasses, etc.). In addition, the ET warper offers the generation and insertion of selective TPS-grids into the 3D mesh in all kind of orientations. Also cutting planes can be used to highlight regions of interest. The protocols for all these applications can be found in the EVAN-Society website. Finally, one can export 3D meshes (.stl, .obj, .ply) of TPS-warped shapes representing the results of given analyses (Bastir *et al.*, 2014). However, these 3D meshes are exported in shape space and thus need to be rescaled accordingly. This export of meshes that represent 3D-GM analyses is particularly useful for the final step in a Virtual Morphology Lab, the 3D printing (Fig. 2). Similar facilities exist in Viewbox 4, which can also warp textures.

### **3D printing of virtual morphological objects and 3D-GM results**

Object manipulation enhances our attention to and improves our comprehension of spatial properties of real-world objects, allowing us to better understand those things we can touch (Turner *et al.*, 2017). Yet, in paleoanthropology, the personal manipulation of fossils, (including touching them with the hands), is limited to very specific situations and partially privileged persons because of the specific scientific value of precious fossils or, sometimes, even rare, historical casts. However, this physical interaction with the object and the knowledge and experience extracted from it are crucially important for morphological research and 3D printing can help in this respect.

Widespread 3D printing is a relatively recent technology. However, in 1980, the idea of rapid prototyping arose and successive models of

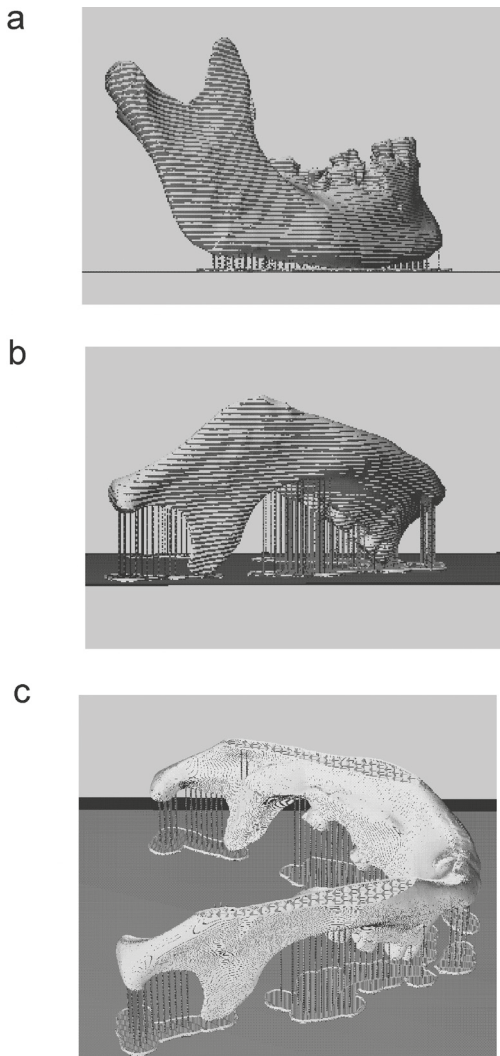


**Fig. 6 - Preview of a 3D print file of a mandible. (a) The natural orientation of the mandible barely needs any support structures. (b) Inverted orientation of the mandible requires many support structures for printing. (c) This view shows all help structures of a 3D print. On the bed the rafts are shown. Rafts are the basis on which the model and the supports are printed. The cutting plane through the 3D model (mandibular corpora and angles) shows the hexagonal geometric pattern of the infill structures that are necessary for robustness of the model and for printing the last layers.**

printing were developed. It was Adrian Bowyer (University of Bath, United Kingdom) who popularized this technique in 2005, under an open source auto-replication robot project called The Replication Rapid-Prototyper Project (RepRap) (Amigo, 2015). After these first initiatives, 3D printing experienced an enormous popularity and 3D printers have now become widely available.

#### *Principles of a 3D printer and printing technologies*

There are different 3D printing technologies available but all of these are based on a fundamental principle that is the deposition of the construction material, layer by layer, one on top of the other, until the object is complete; this is why this technology is called additive construction or additive manufacture. Different 3D printing technology can be distinguished and the most important methods are 1) stereolithography (SLA), 2) selective laser synthesis (SLS), 3) injection printing (IP), and 4) fused deposition model (FDM), among others (Crafts *et al.*, 2015). All these 3D printers evolve at a very fast pace and are suited for different sizes, aims and also produce different final qualities (Crafts *et al.*, 2015; Carew *et al.*, 2019). Depending on the needs one can thus either use this technology via online services (e.g. see the section “Info on the web”), or one can decide to implement a 3D printing lab.

In the Virtual Morphology Lab (MNCN-CSIC) we use FDM technology which is among the most simple, economic, and also most ecological techniques. The FDM or FFF (fused filament fabrication) is the process by which a Cartesian 3D model is constructed through successive 2D layers organized along the z-axis, that is, a process by which a plastic in the form of a molten filament is deposited on top from another to create a 3D object layer by layer. Various thermoplastics are used as raw material, the most frequent being PLA (polylactic acid) and ABS (Acrylonitrile Butadiene Styrene). PLA is a biopolymer composed of lactic acid derived from the fermentation of corn starch or sugarcane. Because of these properties PLA is biodegradable, which is not the case for ABS.

### *The FDM printing process*

The basic parts of an FDM printer consist of the printer head, the rails and the base or bed. The printer head is composed of a stepper motor that drives the filament through a hot zone (hot end, 190 - 220 °C) where it will melt and be extruded through the nozzle (extruder). The movement of the head by the rails deposits the filament on the bed to build the 3D object and therefore any object to be printed is constructed from its basis towards the top. This is also the reason why the first layer is of primary importance determining the rest of the 3D print. It is recommendable to print first a kind of surface, a raft, before the first layer is printed. The raft compensates possible irregularities of the bed surface and guarantees the best possible printing of the first layer. In addition, the raft also provides the necessary adhesion of the entire 3D print during construction. If the print loses its contact with the bed during printing filament will be printed in the air and sooner or later the nozzle will be obstructed. To avoid this sometimes lacquer spray is used to increase the adhesion.

Because in FDM one layer is built on top of another layer of the object some geometric features require printing of additional helping structures (supports), on which consecutive object layers of the overhanging structure can be constructed. For example, a mandible in its natural position can be printed with almost no support structures. This is because all of its maximal dimensions are located at the base or very close to it. Therefore, all object (mandible) layers can be constructed on the basis of the first layer (Fig. 6a; actually, because the corpora are slightly curved very few supports are indeed necessary). However, when for some reasons a mandible is to be printed up-side down (Fig. 6b) then many supports are necessary as some structures (the more distal part of the tooth row, the condyles, the projecting chin, etc.) would otherwise “hang in the air”. For these structures there exists no previous object layer on which other layers could be built. Instead, supporting structures (tiny brittle columns; Fig. 6b) need to be printed from

the bed onwards, to sustain the layers of overhanging mandibular parts in such an orientation. The supports are removed mechanically once the printing is finished. Usually, they are much more brittle than the printed object and can be broken off more or less easily but mostly they leave some traces on the object.

Something similar occurs with the final layer of an object. Because the last layer will close the 3D print and because this closed layer is also printed in horizontal plane (x-y plane) internal supports are needed. Because these supports are printed inside the object they are called “infill”. Without infill no structure could be closed during the last stages of 3D printing. The infill, which is usually a simple geometric pattern (Fig. 6c), gives the model also its physical consistency and will influence in many cases the surface finishes of the top and bottom of the 3D print. Because of this, finding the best position of the model is essential to obtain an optimal result and usually requires some experimentation for the final print. Figure 6c shows all helping structures in detail (the rafts, the supports, and the infill).

In our laboratory, we use three different types of FDM 3D printers, each used because of specific features: the MakerBot Replicator 2 Minireplicators are very easy-to-use and economically affordable direct Cartesian printers. With a building volume of 28.5 x 15.3 x 15.5 cm the Replicator 2 can be used to print many structures of a human skeleton (except complete skulls, some long bones). Because of its straightforward use most of our 3D objects are printed with these machines for a first and quick overview print. (Also the Minireplicators are easy to handle, which is why we use them in the Open Fablab of the MNCN for public workshops for families, children and school classes).

The DeltaWasp40X70 is a fairly fast and large capacity Delta bower printer. With a cylindrical building space of 40 cm diameter and 70 cm height it allows for building large and complex anatomical models such as skulls, fused pelvises, complete rib cages, even full trunk skeletons and all human long bones. This, however, can take considerable time (a thorax in real size takes

**Tab. 2 - Comparison of the 3D printers in the Virtual Morphology Lab (MNCN-CSIC).**

3D PRINTER	BUILD VOLUME (CM)	NOZZLE DIAMATER (MM)	NOZZLE TEMPERATURE (°C)	EXTRUDER	FILAMENT DIAMETER (MM)	MAX LAYER RESOLUTION (MM)	PRINT SPEED (MM/S)
Makerbot Replicator R2	28.5 length 15.3 width 15.5 height	0.4	180-260	single	1.75	0.1	20-140
DeltaWasp	40 diameter (cylindrical print area) 67 height	0.4	180-260	single	1.75	0.1	20-270
Ultimaker 3 Extender	single extrusion: 21.5 length x 21.5 width x 30 height dual extrusion: 19.7length x 21.5width x 30 height	0.4	180-280	double	2.8	0.02	30-300

between 150-190 hours to finish). Also, because of the large size of the printer base a greater number of smaller pieces can be produced in a relatively short time and, above all, in one simultaneous printing process (e.g., the isolated vertebrae and ribs of a thorax).

The Ultimaker3+ Extended is a direct Cartesian printer used to build complex and detailed structures with a building volume of 34 x38 x 49 cm. This 3D printer has two extruders which allows for printing structures in two colors or two different materials. This latter option is interesting for printing highly complex and delicate geometries where the first extruder builds the main object while the second one builds the support structures with a specific material such as Polyvinyl-alcohol (PVA) that is water soluble. Once the 3D print is finished, it is submerged in water and the support structures get dissolved. Apart from producing small models of delicate structures (small-sized rib cages), we use this 3D printer to build 3D models of fossils that require a high definition or internal osteological structures. Its precision along the z-axis (layer height) is lower than that of the others (0.06 mm),

which allows us to make hyper-detailed models. The main technical and practical features of each 3D printer are detailed in Table 2.

#### *Hard- and software set up before printing*

All 3D printers need to be configured before the printing process, with a special focus on different parameters affecting the speed of the process and the quality of the final result. One should configure these parameters following the manufacturer's instructions. Among these parameters, the most important is the adjustment of the height of the bed or the configuration of the z-axis.

Specifically, the z-axis of the Cartesian and of the Delta printer is marked by the surface of the base. This is responsible for establishing a vertical movement that allows builds the object layer by layer. It is necessary to establish an appropriate distance of the nozzle with respect to the bed. This distance must be large enough that it allows for filament extrusion and small enough to guarantee the first layer sticking to the surface. This value is determined by the diameter of the nozzle.

**Tab. 3 - Practical technical details of the 3D printers used in the Virtual Morphology Lab (MNCN-CSIC).**

3D PRINTER	OWN SOFTWARE SLICER	WORK ARCHIVES	BUILD PLATE LEVELING	HOT BED	CONNECTIVITY
<b>Makerbot Replicator R2</b>	MakerbotDeskop	.x3g	manual	no	USB, SD card
<b>DeltaWasp</b>	no	.gcode	manual	0C°-100C°	USB, SD card
<b>Ultimaker 3 Extender</b>	CURA	.gcode	manual/auto	20°C-100C°	USB,wifi, SD card

As a general rule, the maximum resolution/quality along the z-axis that can be reached with a nozzle is 80% of its diameter. For example, if the nozzle diameter is 0.4 mm the maximum layer height (=quality) will be 0.32 mm. Half of the nozzle diameter (approximately 0.16 mm) will be used to establish the initial distance of the nozzle with respect to the base. This parameter is crucial because, as mentioned above, a good 3D printing result depends on the quality of the first layer. This first layer determines the compression between remaining layers and will affect thus the density, dimension and appearance of the entire structure. In summary, the greater the height, the more probable the under-extrusion, whereas the smaller the height, the more probable and over-extrusion. Printing a raft before the first layer will improve these relations (Fig. 6). A good calibration of the z-axis is at the very basis of the printing success. All our printers need a manual calibration but the Ultimaker 3+ carries also out an automatic recalibration.

Once the printer is configured, the some basic parameters of the printing software need to be adjusted. Software packages such as Simplify3D, Slic3r and Cura can be used for these aims. These programs provide a precise control of complexity and personalization of printing parameters (speed, material flow rates, nozzle, retraction, times, etc.). Slic3r and Cura are free programs while Simplify3D is commercial. In our lab we use Simplify3D for generating print files for Makerbot and DeltaWasp printers and Cura to generate print files for the Ultimaker 3+.

Professional printing software (Simplify3D) offers a wide range of parameters that can be edited but usually the most important factors to be considered are: 1) temperature and speed, more related to the thermoplastic material; 2) object-orientation, layer heights, more related to the resolution of the print, and 3) the definition of rafts, support structures and infill, which are more specific to the object and the requirements of finishing quality. The result of these adjustments is a machine-specific print file of the specific 3D object to be printed. If these settings prove successful, it is recommended to store the print file for further repetition of print jobs of this object and material.

The following parameters need to be taken into account and eventually adjusted:

Temperature: Each manufacturer of thermoplastic filament provides the user with a range of recommended temperatures. These parameters are theoretical and can be adjusted slightly depending on the needs of the laboratory, but they give a rough idea of the necessary initial configuration of the print file. For example, an optimal temperature range of PLA is between 190 °C – 230 °C but while Makerbot R2 prefers up to 230 °C, Deltawasp prefers temperatures towards the lower PLA range (190-200°C). The temperature of the environment is also important, particularly if the printers do not offer a chamber in which the 3D print is carried out. Low ambient temperatures affect the adherence and fusion of the layers during printing. Do not open the windows of the lab for ventilation

during cold outside temperatures, and don't forget switching off the air-condition system, when leaving the lab.

**Speed:** Print speed ranges typically between 40 mm/s – 90 mm/s. It is recommendable to start within the lower ranges and then, if necessary, increase. After some experience with the 3D printer, one will be able to determine the optimal printing values for each filament, although these values can be occasionally changed as required by the geometry or size of some models. Geometry is important because organic models have cavities, crests, processes, holes and other complex structures that make their 3D printing more difficult than that of simple geometries (cubes, cylinders, pyramids, etc.). These particularities should be taken into account by adjusting the speed and the temperature. In a region with more details and irregular morphologies (e.g. anterior nasal spine, nasal bones in the skull, coronoid processes of the mandible, the tips of the transverse or spinous processes of vertebrae, canines) reducing the speed can improve quality as the deposition of the molten filament can follow more exactly the complexity of the structures. However, if the printing speed is reduced, it is also necessary to decrease the temperature because higher temperature decreases the viscosity coefficient of the plastic, causing more plastic to be extruded by exerting the same pressure. This phenomenon is known as over-extrusion. The printing speed will also contribute to determine the time the previous layer needs to get solid. A low print speed offers more time for the previously printed layer to cool down before the next one is deposited.

**Orientation of the object:** As mentioned previously, the object is constructed from its basis towards its top. Therefore, each object or 3D print has its preferable orientation which will affect morphologically the location of the support structures and economically the printing time and quantity of the material (mandible in the position shown in Figure 6a takes 2h 30 minutes to print, while in the orientation shown in Figure 6b it takes 3h 26 minutes). As a rule of thumb those structures that can be printed

without supports will have the best possible aspect and finishing. Consequently, the orientation depends on the purpose of the 3D print model or on that part of the model that needs to be highlighted. The slicing software builds the support structures beyond a given angle of the part of the object relative to the bed. In Figure 6b the lower part of the mandibular symphysis (close to the chin) exceeds 45 degrees relative to the build plate. Consequently, supports are printed close to the chin. In turn, the ascending ramus in Figure 6a is always below 45 degrees relative to the build plate. No support is necessary.

A cranium, for example, is best printed in its natural position because the rough surface that remains after removal of the support structures mimics to some degree the morphology of the natural roughness of the muscle and tendon insertions at the cranial base. On the other hand, other orientations will affect other aspects. If the cranium is oriented with the occipital at the base and slightly rotated posteriorly the facial structures will not need any support structures which saves both material and time. Also the physical resistance is affected by the orientation. If forces are likely to be expected from the handling of the 3D print, the orientation of the infill should be in line with the major direction of forces. Finding the best orientation requires some experiments but it is worth trying. When all aspects of the 3D print are important or delicate (e.g. small-sized thorax models) we use double extrusion in the Ultimaker3+ and water soluble PVA filament for supports.

**Nozzle diameter:** Controlling the diameter of the nozzle allows one to influence the quality of the printed piece and to predict the kind of elements that can or cannot be built. This feature is called printability. The printability depends on the diameter of the nozzle and the presence of angular structures in the model. The nozzle influences the layer height and the wall thickness, sometimes also called shells. In the preview of complex objects the slicing software can show gaps between the layers. These gaps show parts that are non-printable because the thickness of the layer in that part of the 3D mesh is less than the diameter of the nozzle. The wall thickness

determines the minimum part of the mesh that will be printed in one run of the extruder, that is, the minimum thickness of one layer.

### *3D printing tips and tricks*

- 1) It is highly recommended to use a filament of good quality even if it is more expensive so that the printing flow is constant and thus avoiding bad results and extruder obstructions.
- 2) Excessively high temperatures (above 230 degrees for standard and PLA nozzles) damage the extruder and carbonize the filament potentially causing obstructions.
- 3) It is recommended to provide a route to the filament before entering the hot end. It is very important to release tensions in the filament to avoid breaks and underextrusions in the model, seen as small gaps, due to the lack of filament in those places. To avoid this, one can place a secondary reel next to the main one. This will cause the filament to wrap before entering bowden tube on the secondary reel by relaxing and unraveling the filament.
- 4) If the company supplies specific software for its own printer, it is recommended to use it because they are adapted to the 3D printer's firmware.
- 5) Check always carefully the preview of the printed model in the software. This is very important to determine its printability.
- 6) The quality of the STL of OBJ model will determine the final result of the 3D printing. Therefore, the pre-processing of the 3D model is very important (smoothing, filling holes, etc.) will improve the quality of the final result.
- 7) To improve the adhesion of the piece to the bed, one can apply adherents such as sprays, lacquer and glue just before printing starts. Sometimes, when printing goes well but the piece loses contact, adhesion tapes can be used to fix the raft on the bed on the go.
- 8) Some supports are necessary to give stability to the piece, especially if it is printed at

high speeds that can lift part of the model from the bed.

- 9) 3D prints with a high probability of base separation or numerous undulations on the surface need lower print speed than those having a large number of straight lines. Adjust the resolution to the size of your print to avoid unnecessary times, for example unless you want to highlight some detail, printing a human skull at 0.2 mm is enough; below this value the aesthetic impression does not increase while wasting a lot of time.

### *Post-processing of 3D prints*

Once the pieces are printed, it is usually necessary to carry out some post-printing treatments to optimize the results. These treatments include the removal of supports (either manually or dissolved in water) and of remains of some unwanted material that may have been deposited on the surfaces the piece. Finally, if the model was printed in different parts, these need to be joined using different methodologies to clean the fitting surface parts (using blades, scalpels, pliers, spatulas, sandpaper, files, rotating tools, etc.). Also more advanced methods can be used such as grit blasting, sandblasting or polishing with abrasives and thermal or chemical treatments.

One important aspect is the generation of a coloured texture (polychroming), which is sometimes necessary to generate an anatomically more realistic impression than the one achieved by the colour of the monochromatic thermoplastic filament. This is particularly important in the context of museum exhibitions. There are two ways to get polychromatic pieces: by obtaining a cast of the 3D printed model that will be polychromed or by the application of a patina directly to the 3D print. Casting of 3D prints is common when used for conservation or expository aims. This is because 3D printing materials have not yet been sufficiently investigated and their ageing properties are still quite unknown. Latest research has shown that the base polymers used in 3D printing and their additives, such as colourants, are highly unstable and therefore its use in exhibitions is not advisable (Coon *et al.*, 2016). On the

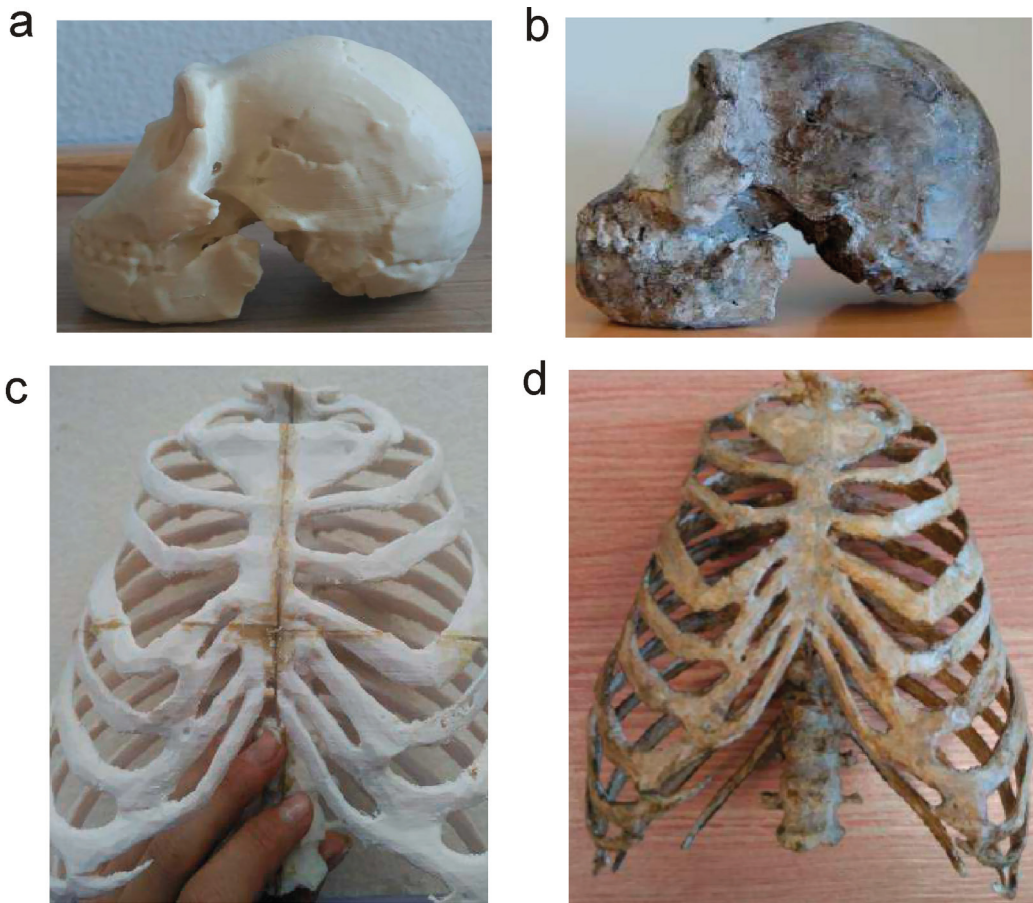


**Fig. 7 - Post-processing and polychromatic staining of 3D prints. (a) 3D PLA print of the *H. naledi* skull. (b) cast of the 3D print that has been stained with natural sediment colours to improve longevity of the colours in exhibitions. (c) Four pieces of PLA printed ribcage glued together (for example necessary when the entire model does not fit the building space). (d) 3D print full rib cage model directly stained with natural sediment colours. The colour version of this figure is available at the JASs website.**

other side, registering an original piece directly by casting is becoming less frequent because of the damage and consequences that this entails for the original. As an example, in our lab we produced a cast of the 3D print of the skull of *Homo naledi* (Fig. 7a) for the paleoanthropological part of exhibition at the MNCN-CSIC (Ávila, 2017). We used silicone to record morphological details of the 3D printed skull and plaster to provide the rigidity where necessary. The mould was

formed in several parts due to the complexity of its shape, and once complete, it was filled with epoxy resin mixed with pigments and other fillers (Santos Gómez, 2005) in order to get a cast with the colours and patina appearance closest to the original possible (Fig. 7b).

Alternatively, it is also possible to apply a patina directly to a 3D print to change its monochromatic appearance. This is the case of the patina applied to a 3D print of a Neandertal

ribcage (Sawyer & Maley, 2005). In this example, we surface-scanned the real size cast of the Neandertal in the MNCN collection and then printed the thorax model half-size and in four pieces using the R2 Makerbots. After the removal of the supports, these four thorax pieces were joined together using different adhesives, such as glue for rigid plastics, a contact glue, super-fast liquid glue based on methyl cyanoacrylate and hot glue applied with a heat gun, according to the size and geometry of the surfaces to be adhered (Fig. 7c). In addition, and to achieve an optimal union between the lower and upper part a pin (i.e. a piece of plastic) was placed in a hole in the centre of the joining surfaces in order to provide greater fixation and support to the 3D print. For a polychromatic colouring of the thorax, a mixture of different pigments was used and agglutinated by matt varnish. The choice of matte quality is important in the reproduction of bones and fossils since they usually do not show any kind of brightness. The piece was coloured directly with the mixture applied with a brush (Fig. 7d) (Ávila, 2017).

## Discussion

This review has presented standard workflows and methods in virtual morphology which are relatively easy to implement as a laboratory in academic institutions and useful in various respects of anatomical and morphological research. The methods outlined here facilitate comparative morphological research because once museum specimens are properly digitized they can be made available to a wide range of students and researchers as exemplified recently in the form of digital databases (see some example listed in section *Databases on the internet*). Consequently, these technologies reduce research costs by avoiding the need for traveling, curation and protection. In addition, broad access to data enhances the speed of scientific progress as more researchers are investigating these objects.

In palaeoanthropology, fossil specimens are usually compared with greater comparative

samples of extant species using 3D-GM (e.g. Williams *et al.*, 2017; Neubauer *et al.*, 2018). Accordingly, more and more fossil data are actually digitally available either via the just mentioned digital data bases, or via 3D models directly downloadable from the corresponding publication site (Weaver & Hublin, 2009) or accessible online, virtually, by interactive manipulation of the 3D image (Bastir *et al.*, 2014). However, regarding recent species it is currently still quite difficult to get a reasonably sized comparative data set allowing for statistically robust 3D-GM analyses. Efforts in both, fostering mass digitisation and standardizing digitisation quality criteria, are currently part of the EU research policy in Natural Sciences (e.g. SYNTHESYS+; DISCCO, etc.). Such conversion of physical into digital collections will reduce this problem by leading to improved and widely accessible data bases for research activities at both student and professional levels.

These digital 3D models enter directly into the 3D-GM toolkit for statistical analyses and interactive 3D visualizations. Importantly, while several software packages are available for 3D-GM analyses (see **Measurement of 3D meshes (landmarks, semilandmarks of curves and surfaces)**), the use of open access code in R is increasingly used leading to fast and innovative development of further analytical protocols for the intersection between pure 3D-GM and virtual morphological treatment of 3D images (Profico *et al.*, 2016).

As shown in this paper, the dramatic development in 3D printing now offers the opportunity to 3D-print the results of the 3D-GM analyses with very little costs. This offers new opportunities in palaeoanthropology, or more generally, palaeontological sciences, where the reconstruction of incomplete fossils is an important step. With 3D printing fossil reconstructions based on 3D-GM or other virtual morphological work can be produced for physical inspection. Such reconstructions could even be re-introduced in existing cast collections of academic institutions and studied using traditional morphometric methods (Carew *et al.*, 2019).

Here, one important remark should be mentioned. 3D printing of human remains should follow ethical considerations regarding respect and dignity. Such considerations are particularly relevant in the context of anatomical teaching or forensics and less so in a paleoanthropological context and no clear guidelines are currently elaborated (Márquez-Grant & Errickson, 2017). Ethical consideration is even more important when 3D prints are to be shared and, thus, multiplied and distributed.

Although 3D prints of virtual anatomical objects do not actually present new data, they do stimulate new intellectual channels of perception of the researcher leading to enhanced attention to the object. This is related to the “power of things”, the haptic interaction between the physical object and the researcher. It can lead to a better comprehension of complex 3D anatomy, its variation and evolutionary change and also stimulate creative processes for further research or experiments.

These very same psychological principles apply to teaching and learning in Natural History Museums. 3D scanning and printing technology overcome the limitation that exists due to prohibition for visitors to touch or manipulate original pieces of exhibition. When implemented in Museum workshops (e.g. palaeontology, comparative anatomy, or, more generally, natural sciences) children can benefit following recent educational trends in museology (STEAM-methods, Stein *et al.*, 2016; Turner *et al.*, 2017). Finally, to some extent 3D technology can facilitate certain aspects of social inclusion into museology, of people which for different reasons due to physical or mental handicaps will benefit from direct manipulations with 3D printed objects of exhibition of both art and natural science context.

## Acknowledgements

*Funding: CGL2015-63648-P (MINECO), SYS 3, and FCT-17-12123 (FECYT). Two reviewers provided very helpful comments to previous versions of the manuscript.*

## Info on the web

<http://www.nextengine.com/>  
[www.artec3d.com/](http://www.artec3d.com/)  
*Scanning devices.*

<https://www.youtube.com/watch?reload=9&v=4VPfrLlFRWc>  
*Scanning tutorial.*

<http://www.3d-microscribe.com>  
<http://pages.nycep.org/nmg/programs.html>  
[www.dhal.com](http://www.dhal.com)  
<http://graphics.idav.ucdavis.edu>  
*Digitization software.*

<http://www.r-project.org/>  
 Geomorph: <https://cran.r-project.org/web/packages/geomorph/index.html>  
 Morpho: <https://www.r-project.org/nosvn/pandoc/Morpho.html>  
*R project.*

<http://www.evan-society.org/>  
*Evan-Society website.*

<https://www.materialise.com/en/manufacturing/3d-printing-technology>  
[www.shapeways.com](http://www.shapeways.com)  
[www.i.materialize.com](http://www.i.materialize.com)  
<http://hubspot.3dhubs.com>  
*3D printing.*

[www.disco.eu](http://www.disco.eu)  
*Others.*

## References

- AbouHashem Y., Dayal M., Savanah S. *et al.* 2015. The application of 3D printing in anatomy education. *Med. Educ. Online*, 20: 29847.
- Adams D. C., Collyer M. L. & Kaliontzopoulou A. 2019. *Geomorph: Software for geometric morphometric analyses. R package version 3.1.0.*

- Amigo D. 2015. *Guía de post-procesado de modelos digitales para la impresión 3D y prototipado anatómico*. Trabajo fin de grado, Universidad de Alcalá.
- Bastir M., O'Higgins P. & Rosas A. 2007. Facial ontogeny in Neanderthals and modern humans. *Proc. R. Soc. Lond. B*, 274: 1125-1132.
- Bastir M., Rosas A., Gunz P. et al. 2011. Evolution of the base of the brain in highly encephalized human species. *Nat. Commun.*, 2: 588.
- Bastir M., Higuero A., Ríos L. et al. 2014. Three-dimensional analysis of sexual dimorphism in human thoracic vertebrae: Implications for the respiratory system and spine morphology. *Am. J. Phys. Anthropol.*, 155: 513-521.
- Bastir M. & Rosas A. 2016. Cranial base topology and basic trends in the facial evolution of Homo. *J. Hum. Evol.*, 91: 26-35.
- Bastir M. 2018. Back to Basics: Morphological Analysis in Paleoanthropology In J. Schwartz (ed): *Biological Theory*, pp: 205-227. MIT-press, Boston.
- Bastir M., Torres-Tamayo N., Palancar C.A. et al. 2019. Geometric Morphometric Studies in the Human Spine. In E. Been, A. Gómez-Olivencia & P.A. Kramer (eds): *The human spine*. Springer Verlag (in press).
- Berger L.R., Hawks J., de Ruiter D.J. et al. 2015. Homo naledi, a new species of the genus Homo from the Dinaledi Chamber, South Africa. *eLife*, 4: e09560
- Bruner E. & Bastir M. 2008. Digital Morphology: modelling anatomy and evolution. *J. Anthropol. Sci.*, 86: 3-5.
- Bookstein F.L. 1991. *Morphometric tools for landmark data*. Cambridge University Press, Cambridge.
- Bookstein F.L. 1996. Combining the tools of geometric morphometrics. In L.F. Marcus, M. Corti, A. Loy, G.J.P. Naylor & D.E. Slice (eds): *Advances in morphometrics*, pp. 131-151. Springer, Boston.
- Bookstein F.L. 1997. Landmark methods for forms without landmarks: morphometrics of group differences in outline shape. *Med. Image Anal.*, 1: 225-243.
- Bookstein F.L., Sampson P.D., Connor P.D. et al. 2002. Midline corpus callosum is a neuro-anatomical focus of fetal alcohol damage. *Anat. Rec.*, 269: 162-174.
- Bookstein F.L., Gunz P., Mitteroecker P. et al. 2003. Cranial integration in Homo: singular warps analysis of the midsagittal plane in ontogeny and evolution. *J. Hum. Evol.*, 44: 167-187.
- Bookstein F.L. 2017. A method of factor analysis for shape coordinates. *Am. J. Phys. Anthropol.*, 164: 221-245.
- Boyer D.M., Gunnell G.F., Kaufman S. et al. 2016. Morphosource: Archiving and sharing 3-d digital specimen data. *Paleobiology*, 22: 157-181.
- Canessa E., Fonda C., Zennaro M. et al. 2013. Low-cost 3D printing for science, education and sustainable development. *Low-Cost 3D Printing*, 11.
- Carew R.M., Morgan R.M. & Rando C. 2019. A Preliminary Investigation into the Accuracy of 3D Modeling and 3D Printing in Forensic Anthropology Evidence Reconstruction. *J. Forensic Sci.*, 64: 342-352.
- Catanzaro M. 2010. Austerity measures sap Spanish science. *Nature*, 10.1038/news.2010.520
- Cignoni P., Callieri M., Corsini M. et al. 2008. MeshLab: an Open-Source Mesh Processing Tool. *Eurographics Italian*, 2008: 129-136.
- Coon C., Pretzel B., Lomax T. et al. 2016. Preserving rapid prototypes: a review. *Herit. Sci.*, 4: 40.
- Copes L.E., Lucas L. M., Thostenson J.O. et al. 2016. A collection of non-human primate computed tomography scans housed in MorphoSource, a repository for 3D data. *Sci. Data*, 3: 160001.
- Conroy G.C., Weber G.W., Seidler H. et al. 1998. Endocranial Capacity in an Early Hominid Cranium from Sterkfontein, South Africa. *Science*, 280: 1730-1731.
- Dedouit F., Telmon N., Costagliola R. et al. 2007. Virtual anthropology and forensic identification: report of one case. *Forensic Sci. Int.*, 173: 182-187.
- Dryden I.L. & Mardia K.V., 1998. *Statistical Shape Analysis*. Wiley, Chichester, England.
- EVAN-Society. 2010. ET, Toolkit for geometric morphometric analysis.
- Fajardo R.J. & Müller R. 2001. Three-dimensional analysis of nonhuman primate trabecular

- architecture using micro-computed tomography. *Am. J. Phys. Anthropol.*, 115: 327-336.
- Fau M., Cornette R. & Houssaye A. 2016. Photogrammetry for 3D digitizing bones of mounted skeletons: Potential and limits. *Comptes. Rendus. Palevol.*, 15: 968-977.
- Friess M. 2012. Scratching the surface? The use of surface scanning in physical and paleoanthropology. *J. Anthropol. Sci.*, 90: 7-31.
- García-Martínez D., Nalla S., Ferreira M.T. *et al.* 2018. Eco-geographic adaptations in the human ribcage throughout a 3D geometric morphometric approach. *Am. J. Phys. Anthropol.* 166: 323-336.
- García-Martínez D. 2017. *Contributions to the study of the morphological, functional and evolutionary variability of the human rib cage*. PhD dissertation, Universidad Autónoma de Madrid.
- Gower J.C. 1975. *Generalized procrustes analysis*. *Psychometrika*, 40: 33-51.
- Guidi G., Russo M. & Angheluddu D. 2014. 3D survey and virtual reconstruction of archeological sites. *DAACH*, 1: 55-69.
- Gunz P., Mitteroecker P. & Bookstein F.L. 2005. Semilandmarks in three dimensions. In D.E. Slice (ed): *Modern morphometrics in physical anthropology*, pp. 73-98. Springer, US.
- Gunz P., Mitteroecker P., Neubauer S. *et al.* 2009. Principles for the virtual reconstruction of hominin crania. *J. Hum. Evol.*, 57: 48-62.
- Gunz P. & Mitteroecker P. 2013. Semilandmarks: a method for quantifying curves and surfaces. *HYSTRIX*, 24: 103-109.
- Hammer Ø. 2015. *PAST: Paleontological Statistics. Reference Manual*. Natural History Museum, University of Oslo. Oslo, Norway.
- Jones N. 2012. Science in three dimensions: the print revolution. *Nature News*, 487: 22.
- Katz D. & Friess M. 2014. Technical note: 3D from standard digital photography of human crania - A preliminary assessment. *Am. J. Phys. Anthropol.*, 154: 152-158.
- Kendall D.G. 1977. The diffusion of shape. *Adv. Appl. Probab.*, 9: 428-430.
- Klingenberg C.P. 2011. MorphoJ: an integrated software package for geometric morphometrics. *Mol. Ecol. Resour.*, 11: 353-357.
- Kullmer O. 2008. Benefits and risks in virtual anthropology. *J. Anthropol. Sci.*, 86: 205-207.
- Lim K.H.A., Loo Z.Y., Goldie S.J. *et al.* 2016. Use of 3D printed models in medical education: a randomized control trial comparing 3D prints versus cadaveric materials for learning external cardiac anatomy. *Anat. Sci. Educ.*, 9: 213-221.
- Maret D., Molinier F., Braga J. *et al.* 2010. Accuracy of 3D reconstructions based on cone beam computed tomography. *J. Dent. Res.*, 89: 1465-1469.
- Márquez-Grant N. & Errickson D. 2017. Ethical considerations: An added dimension. In T. Thompson & D. Errickson (eds): *Human remains: Another dimension*, pp. 193-204. Academic Press.
- Mikhail E.M., Bethel J.S. & McGlone J.C. 2001. *Introduction to modern photogrammetry*. Wiley, New York.
- Mitteroecker P. & Gunz P. 2009. Advances in Geometric Morphometrics. *Evol. Biol.*, 36: 235-247.
- Neubauer S., Gunz P., Leakey L. *et al.* 2018. Reconstruction, endocranial form and taxonomic affinity of the early Homo calvaria KNM-ER 42700. *J. Hum. Evol.*, 121: 25-39.
- Niven L., Steele T.E., Finke H. *et al.* 2009. Virtual skeletons: using a structured light scanner to create a 3D faunal comparative collection. *J. Archaeol. Sci.*, 36: 2018-2023.
- O'Higgins P. & Jones N. 1998a. Facial growth in *Cercocebus torquatus*: An application of three-dimensional geometric morphometric techniques to the study of morphological variation. *J. Anat.*, 193: 251-272
- O'Higgins P. & Jones N. 1998b. Morphologika: a program for the analysis of 3-dimensional shape variation using landmarks. <https://sites.google.com/site/hymfme/downloadmorphologica>.
- O'Higgins P. 2000. The study of morphological variation in the hominid fossil record: biology, landmarks and geometry. *J. Anat.*, 197: 103-120.
- O'Higgins P. & Jones N. 2006 *Tools for statistical shape analysis*. Hull York Medical School.
- O'Higgins P., Cobb S.N., Fitton L.C. *et al.* 2011. Combining geometric morphometrics and

- functional simulation: an emerging toolkit for virtual functional analyses. *J. Anat.*, 218: 3-15.
- Pain E. 2012. Research Cuts Will Cause 'Exodus' From Spain. *Science*, 336: 139-140.
- Ponce De León M.S., Golovanova L., Doronichev V. et al. 2008. Neanderthal brain size at birth provides insights into the evolution of human life history. *Proc. Natl. Acad. Sci. USA*, 105: 13764-13768.
- Profico A., Di Vincenzo F., Gagliardi L. et al. 2016. Filling the gap. Human cranial remains from Gombore II (Melka Kunture, Ethiopia; ca. 850 ka) and the origin of *Homo heidelbergensis*. *J. Anthropol. Sci.*, 94: 1-24.
- R Development Core Team. 2011. R Language Definition, version 2.132. URL <http://www.r-project.org/>.
- Recheis W., Weber G. W., Schäfer K. et al. 1999. Virtual reality and anthropology. *Eur. J. Radiol.*, 31: 88-96.
- Rodriguez-Perez F.J., Rosas A., García-Martínez D. et al. 2017. A 3D form comparative analysis of the Neandertal glenoid fossa in the context of the genus *Homo*. *Quat. Int.*, 481: 91-10
- Rohlf F.J. & Slice D. 1990. Extensions of the Procrustes method for the optimal superimposition of landmarks. *Syst. Biol.*, 39: 40-59.
- Rohlf F.J. & Corti M. 2000. The use of partial least-squares to study covariation in shape. *Syst. Biol.*, 49: 740-753.
- Santos-Gómez S. 2005. *Las preparaciones de yeso en la pintura sobre tabla de la escuela española*. Universidad Complutense de Madrid, Tesis Doctoral (Madrid), Directora Margarita San Andrés Moya.
- Sampson P.D., Bookstein F.L., Sheehan F.H. et al. 1996. Eigenshape analysis of left ventricular outlines from contrast ventriculograms. In L.F. Marcus, M. Corti, A. Loy, G.J.P. Naylor & D.E. Slice (eds): *Advances in morphometrics*, pp. 211-233. Springer, Boston, MA.
- Sawyer G.J. & Maley B. 2005. Neanderthal reconstructed. *Anat. Rec. B New Anat.*, 283: 23-31.
- Schlager S. 2017. Morpho and Rvcg – Shape Analysis in R. In G. Zheng, S. Li & G. Székely (eds): *Statistical Shape and Deformation Analysis*, pp. 217–256. Academic Press.
- Sellers W., Manning P., Lyson T. et al. 2009. Virtual palaeontology: gait reconstruction of extinct vertebrates using high performance computing. *Palaeontol. Electronica*, 12: 11A.
- Seiffert E.R., Gunnell G.F., Heritage S.W. et al. 2016. Open access to Fayum primate fossils through the digital data archive MorphoSource. *Am. J. Phys. Anthropol.* 159: 286-287.
- Sheets D.H., Kim K. & Mitchel C.E. 2004. A combined Landmark and Outline-Based Approach to Ontogenetic Shape Change in the Ordovician Trilobite *Triarthrus becki*. In A. Elewa (ed): *Morphometrics in Paleontology*. Springer, Berlin, Wien.
- Slice D.E. 2000. *Morpheus et al.: software for morphometric research (Version Revision 01-01-2000)*. Department of Ecology and Evolution, State University, Stony Brook, New York.
- Stein R., Etre K., Farek E. et al. 2016. *Steam initiatives at the carlos museum: Bringing science into the galleries and cultural heritage into the classroom*. Materials Science and Technology Conference and Exhibition, pp. 833-838.
- Spoor F., Wood B. & Zonneveld F. 1994. Implications of early hominid labyrinthine morphology for evolution of human bipedal locomotion. *Nature*, 369: 645-648.
- Toro Ibacache M.V., Manriquez-Soto G. & Suazo-Galdames I. 2010. Morfometría geométrica y el estudio de las formas biológicas: de la morfología descriptiva a la morfología cuantitativa. *Int. J. Morphol.*, 28: 977-990.
- Torres-Tamayo N., García-Martínez D., Nalla S. et al. 2018. The torso integration hypothesis revisited in *Homo sapiens*: Contributions to the understanding of hominin body shape evolution. *Am. J. Phys. Anthropol.*, 167: 777-790.
- Turner H., Resch G., Southwick D. et al. 2017. Using 3D Printing to Enhance Understanding and Engagement with Young Audiences: Lessons from Workshops in a Museum. *The Museum Journal* 60: 311-333.
- Veneziano A., Landi F. & Profico A. 2018. Surface smoothing, decimation, and their effects on 3D biological specimens. *Am. J. Phys. Anthropol.*, 166: 473-480.
- Weaver T.D. & Hublin J-J. 2009. Neandertal birth canal shape and the evolution of human childbirth. *Proc. Natl. Acad. Sci. USA*, 106: 8151-8156.

- Weber G.W. 2001. Virtual Anthropology (VA): A Call for Glasnost in Paleoanthropology. *Anat. Rec.*, 265: 193-201.
- Weber G.W., Schäfer K., Prossinger H. *et al.* 2001. Virtual anthropology: the digital evolution in anthropological sciences. *J. Physiol. Anthropol. Appl. Human. Sci.*, 20: 69-80.
- Weber G.W. 2015. Virtual Anthropology. *Am. J. Phys. Anthropol.*, 156: 22-42.
- Weber G.W. & Bookstein F.L. 2017. *Virtual anthropology: a guide to a new interdisciplinary field*. Springer.
- Williams S.A., García-Martínez D., Bastir M. *et al.* 2017. The vertebrae and ribs of *Homo naledi*. *J. Hum. Evol.*, 104: 136-154.
- Zelditch M.L., Swiderski D.L., Sheets H.D. *et al.* 2012. *Geometric Morphometrics for Biologists: A Primer* (2<sup>nd</sup> edition). Elsevier Academic Press, San Diego.
- Zollikofer C.P.E., Ponce de León M.S., Martin R.D. *et al.* 1995. Neanderthal computer skulls. *Nature*, 375: 283-285.
- Zollikofer C. & Ponce de Leon M. 2005. *Virtual Reconstruction: a primer in computer-assisted paleontology and biomedicine*. John Wiley & Sons, Hoboken, New Jersey.

Editor, Giovanni Destro Bisol



This work is distributed under the terms of a Creative Commons Attribution-NonCommercial 4.0 Unported License <http://creativecommons.org/licenses/by-nc/4.0/>